DCE-MRI定量灌注参数鉴别直肠癌区域淋巴结良恶性的初步探讨

杨心悦[1]，陈 琰[1]，肖晓娟[2]，杨艳红[1]，文自强[1]，卢宝兰[1]，余深平[1]
(1. 中山大学附属第一医院放射科，广东 广州 510080；2. 北京大学深圳医院放射科，广东 深圳 518036)

摘 要：【目的】采用DCE-MRI定量灌注参数评价直肠癌区域淋巴结，以探究各参数鉴别良恶性淋巴结的临床应用价值。【方法】收集本院2015年1月至2016年8月行术前DCE-MRI扫描且未经新辅助治疗行直肠癌根治术患者122例，纳入术前DCE-MRI与术后病理相对应淋巴结203枚(阳性95枚，阴性108枚)，测量各淋巴结短径(S)、长径(L)并计算二者比值(S/L)，测算各淋巴结定量灌注参数，包括对比剂容积转换常数(K_{trans})、速率常数(K_{ep})、单位体积组织细胞外血管外间隙容量(V_e)。比较分析良恶性淋巴结各相关参数，并以S=5 mm为界值，进一步分组比较不同短径下良恶性淋巴结各定量灌注参数；绘制相关定量灌注参数的ROC曲线，获取诊断界值。【结果】转移淋巴结的短径(S)及长径(L)高于非转移淋巴结(P<0.01)，S/L及K_{trans}、K_{ep}则低于非转移淋巴结(P<0.01)，而两组间V_e无统计学差异(P=0.308)，K_{trans}鉴别良恶性淋巴结的诊断界值(曲线下面积，敏感度，特异度)为0.088 min^{-1}(0.69，58.3%，78.9%)。分组分析显示，当S≥5 mm时，转移淋巴结K_{trans}、K_{ep}低于非转移淋巴结(P<0.001)，V_e则高于非转移淋巴结(P=0.039)，K_{trans}鉴别二者的诊断界值(曲线下面积，敏感度，特异度)为0.088 min^{-1}(0.675，57.1%，77.9%)；当S<5 mm时，转移淋巴结K_{trans}低于非转移淋巴结(P=0.001)，其诊断界值(曲线下面积，敏感度，特异度)为0.087 min^{-1}(0.732，60.5%，81.5%)，而两组间K_{ep}、V_e则无统计学差异(P>0.10)。【结论】DCE-MRI定量灌注参数K_{trans}可用于鉴别直肠癌区域淋巴结的良恶性，且K_{trans}在鉴别短径较小(S<5 mm)的淋巴结方面具有一定优势。

关键词：直肠癌；淋巴结；磁共振灌注成像；微血管灌注
中图分类号：R445.2 **文献标志码：**A **文章编号：**1672-3554(2017)06-0909-07

Discrimination between Metastatic and Non-metastatic Regional Lymph Nodes in Rectal Cancer Using Quantitative Dynamic Contrast-enhanced Parameters

YANG Xin-yue[1], CHEN Yan[1], XIAO Xiao-juan[2], YANG Yan-hong[1], WEN Zi-qiang[1], LU Bao-lan[1],YU Shen-ping[1]
(1. Department of Radiology, The First Affiliated Hospital, Sun Yat-Sen University, Guangzhou 510080, China; 2. Department of Radiology, Shenzhen Hospital, Peking University, Shenzhen 518036, China)
Corresponding to: YU Shen-ping, E-mail: ethan_yu@sina.com

Abstract:【Objective】To investigate the diagnostic value of quantitative perfusion parameters of dynamic contrast-enhanced imaging for discriminating metastatic from non-metastatic regional lymph nodes in rectal cancer.【Methods】122 patients of our department were collected from 2015.01 to 2016.08, and 203 lymph nodes, including metastatic lymph nodes (MLNs, n=95) and non-metastatic lymph nodes (NMLNs, n=108), were analyzed. The short-axis diameter (S), long-axis diameter (L), short- to long-axis diameter ratio (S/L), volume transfer constant (K_{trans}), rate constant (K_{ep}) and extravascular extracellular space (EES) fractional volume (V_e) were compared between two groups respectively. Then using S=5 mm as a cutoff value, these parameters were compared between subgroups. Receive operating characteristic curve (ROC) was used to analyze the diagnostic efficiency and find the optimal cutoff values.【Results】The metastatic group exhibited higher S and L, but lower S/L, K_{trans} and K_{ep} than the non-metastatic group (P<0.01). However, the V_e did not differ significantly between two groups (P=0.308). Optimal cutoff values [area under the curve (AUC), sensitivity, specificity] of K_{trans} for discriminate metastatic lymph nodes from non-metastatic were 0.088 min^{-1} (0.69, 58.3%, 78.9%). When S>/=5 mm, subgroup analysis revealed that K_{trans} and K_{ep} of MLNs were significant higher than those of NMLNs (P<0.001), but V_e was lower (P=

收稿日期：2017-08-23
基金项目：广东省科技计划项目(2014A020212126)
作者简介：杨心悦，硕士研究生，研究方向：医学影像学，E-mail：yangxinyue1991@126.com；余深平，通信作者，主任医师，硕士生导师，研究方向：医学影像学，E-mail：ethan_yu@sina.com

0.039). Optimal cutoff values (AUC, sensitivity, specificity) of K_{trans} were 0.088 min^{-1} (0.675, 57.1%, 77.9%). However, when S<5 mm, MLNs showed lower K_{trans} than NMLNs (P=0.001), but there were no significantly statistic differences of K_{ep} and V_e between these two groups (P>0.1). Optimal cutoff values (AUC, sensitivity, specificity) of K_{trans} were 0.087 min^{-1} (0.732, 60.5%, 81.5%).【Conclusion】K_{trans} can be used to discriminate regional MLNs from NMLNs in rectal cancer, especially when the short-axis diameter is less than 5 millimeters.

Key words: rectal cancer; lymph nodes; magnetic resonance perfusion imaging; microvascular perfusion

[J SUN Yat-sen Univ(Med Sci),2017,38(6):809-915]

结直肠癌为全球常见的消化道恶性肿瘤之一[1],其在我国的发病率逐年升高[2],且以直肠癌为著。因直肠癌区域淋巴结转移与治疗方案及疾病预后密切相关[1],故治疗前准确评估区域淋巴结尤为重要。淋巴结评估的传统影像手段主要包括经直肠超声(endorectal ultrasound, EUS)、CT及MRI,但仅依据形态学改变,尚不足以准确诊断淋巴结转移[3]。扩散加权成像(diffusion weighted imaging, DWI)虽能提高直肠癌转移淋巴结的检出率,但ADC值在鉴别淋巴结良恶性上仍存在重叠,尤其是在鉴别较小的淋巴结方面[4]。近年来,随着动态对比增强磁共振成像(dynamic contrast-enhanced MRI, DCE-MRI)的兴起,相关定量灌注参数如血浆与血管外细胞外间隙(extravascular extracellular space, EES)间的对比剂容积转换常数(volume transfer constant, K_{trans})、EES与血浆间的对比剂回流速率常数(rate constant, K_{ep})及单位体积组织的EES容量(EES fractional volume, V_e)因可无创反映组织的微循环情况[5],逐步应用于评价直肠癌病理分级、TNM分期及新辅助治疗效果[6-7],但应用于鉴别直肠癌区域淋巴结良恶性的研究则较少。本研究拟采用DCE-MRI Tissue 4D后处理技术,测定直肠癌DCE-MRI区域淋巴结定量灌注参数K_{trans}、K_{ep}及V_e,探讨各参数鉴别淋巴结良恶性的应用价值。

1 材料与方法

1.1 研究对象

收集中山大学附属第一医院2015年1月至2016年8月胃肠外科收治122例直肠癌患者的临床资料,其中男68例,女54例,平均年龄(59±11)岁。患者纳入标准为:①行直肠癌根治术;②术前未接受新辅助治疗;③术前行DCE-MRI检查;④术中记录清扫淋巴结部位并编号送检;⑥此前未接受过盆腔手术。所有患者均自愿接受直肠MR检查并签署知情同意书。

1.2 MR检查方法

1.2.1 MR扫描设备及常规扫描方案 采用德国Siemens公司Magnetom Verio 3.0T超导型MR成像仪,并选择8通道体部相控阵线圈。MR常规扫描方案包括:①常规横断位T2WI(层厚5.0 mm);②高分辨矢状位、冠状位及正交轴位T2WI(层厚3.0 mm),其中正交轴位T2WI定位垂直于肿瘤所在肠壁扫描。

1.2.2 DCE-MRI扫描方案 常规扫描结束后,行T1 Mapping扫描及DCE-MRI扫描。扫描方案包括:①正交轴位3D双翻转角(2°和15°)Vibe-T1WI(TR 5.08 ms,TE 1.74 ms,FOV 260 mm×260 mm,层厚3.6 mm,体素1.9 mm×1.4 mm×3.6 mm);②正交轴位3D-twist-T1WI(TR 4.83 ms,TE 1.87 ms,FOV 260 mm×260 mm,层厚3.6 mm,体素2.0 mm×1.4 mm×3.6 mm,翻转角12°);③高分辨正交轴位压脂增强T1WI(层厚3.0 mm);④冠状位压脂增强3D-Vibe-T1WI(FOV 380 mm×380 mm,层厚1.0 mm)。

采用3D-twist-T1WI行DCE-MRI扫描时,于5期动态扫描后以高压注射器经肘静脉团注对比剂Gd-DTPA,注射剂量为0.1 mmol/kg,注射速率为3.0 mL/s,注射对比剂后以同样速率注射0.9%生理盐水25 mL,共行75期不间断动态扫描。DCE-MRI扫描定位同常规序列正交轴位相同。扫描前10~15 min所有患者肌注山莨菪碱20 mg以抑制小肠蠕动,减少其运动伪影。

1.3 资料分析

1.3.1 MRI数据处理 应用MR后处理工作站(Syngo MultiModality Workplace, VE40A, Siemens)的Tissue 4D软件对DCE-MRI进行后处理。具体步骤包括:①利用Tissue 4D软件对高分辨T2WI及DCE-MRI进行同层面图像校准;②选择某一枚区域淋巴结最大层面,结合高分辨T2WI确定淋巴

结边缘，测量其短径（Short-axis diameter，S）及长径（Long-axis diameter，L），并避开肉眼可见的坏死区域手动勾画感兴趣区（region of interest，ROI），生成时间-强化曲线（time-relative enhancement curve，TIC）；③根据ROI内血流特点，依次匹配软件内的“Fast”、“Intermediate”及“Slow”动脉输入函数（arterial input function，AIF）模型，选择卡方值最小的模型进行拟合；④生成伪彩图并计算ROI定量灌注参数K_{trans}、K_{ep}及V_e的值，保存后处理图像并记录各参数值；⑤逐层勾画扫描所见该淋巴结全层面，选择最大层面AIF模型进行拟合，重复步骤④；⑥重复步骤②至步骤⑤，勾画扫描范围所见全直肠癌区域淋巴结。

1.3.2　病理资料分析　纳入患者均在行DCE-MRI扫描后2周后内（中位时间间隔5 d，时间间隔范围1～14 d）接受直肠癌根治术，术中依次清扫区域淋巴结，包括中央组、中间组、肠旁组、肠上组、直肠系膜组，按组摆放淋巴结并编号送病理检查。经苏木素-依红染色（hematoxylin-eosin staining，HE染色）辅以免疫组织化学（immunohistochemistry，IHC）技术，判定送检淋巴结良恶性。术后由2位有经验的放射科医师一同根据手术记录及病理结果，结合淋巴结分布区域，再次对DCE-MRI进行阅片，确定扫描范围所见可与病理结果相匹配的淋巴结，将其相关参数纳入统计分析。

1.4　统计学分析

应用SPSS 20.0统计软件进行统计学分析。对淋巴结相关参数S、L、短径/长径（short- to long-axis diameter ratio，S/L）及定量灌注参数K_{trans}、K_{ep}、V_e进行正态性检验；进一步以S=5 mm为界值，分别对S≥5 mm及S<5 mm淋巴结各参数进行正态性检验。S<5 mm淋巴结K_{trans}值符合正态分布，采用两独立样本t检验比较分析；其余各组数据则为偏态分布，均采用两独立样本秩和检验比较分析。以$P<0.05$为差异有统计学意义。绘制受试者工作特征曲线（receive operating characteristic curve，ROC）分析相关定量灌注参数的诊断效能，并求得相应诊断界值。

2　结　果

2.1　淋巴结DCE-MRI与病理检查配准

122名患者（TMN分期分布如下：Tis n=2，T1 n=5，T2 n=27，T3 n=32，T4 n=56；N0 n=69，N1

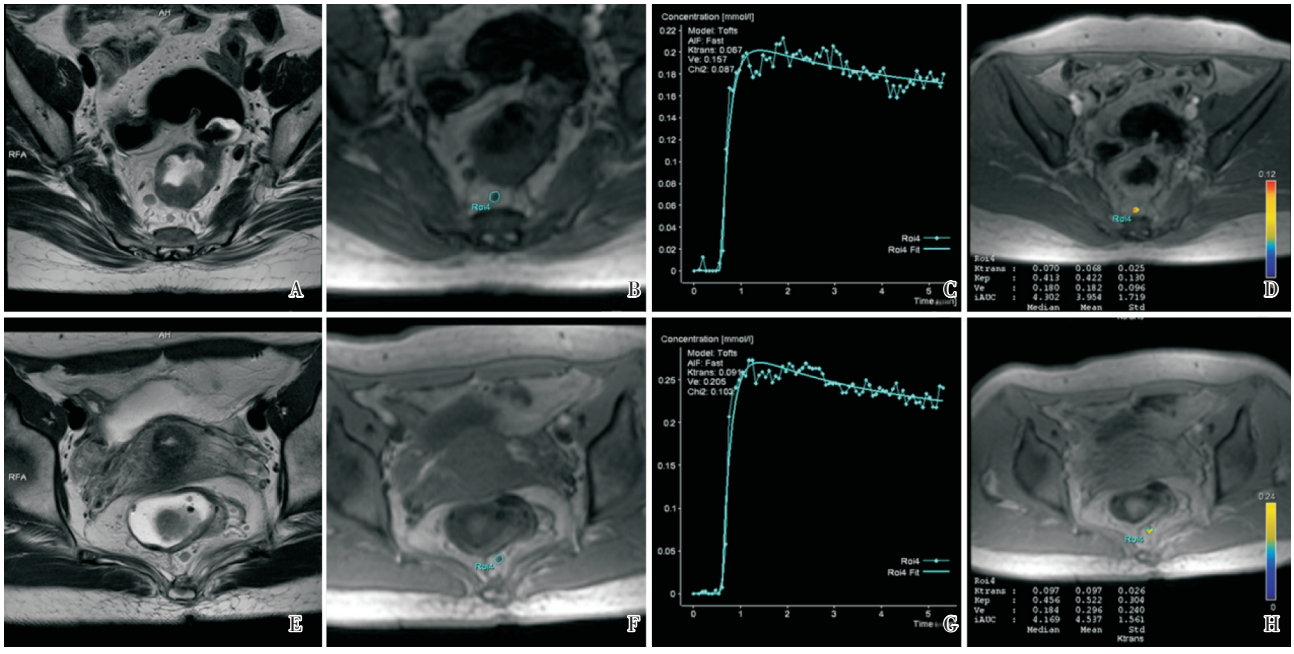

（A）～（D）DCE-MRI analyses of a metastatic lymph node.（A）T2WI of the widest slice；（B）ROI of the widest slice；（C）AIF of ROI；（D）K_{trans} map and parameters.（E）～（H）DCE-MRI analyses of a non-metastatic lymph node.（E）T2WI of the widest slice；（F）ROI of the widest slice；（G）AIF of ROI；（H）K_{trans} map and parameters。

图1　直肠癌区域淋巴结DCE-MRI图像分析与参数测定

Fig.1　DCE-MRI analyses and parametric measurement of regional lymph nodes in rectal cancer

表1 转移与非转移淋巴结径线及定量灌注参数比较

Table 1 Size and quantitative perfusion parameters of metastatic and non-metastatic lymph nodes

Parameter	Metastatic LNs (n=95)		Non-metastatic LNs (n=108)		U	P
	Median	IQR	Median	IQR		
S/mm	5.99	3.51	5.39	1.91	3730	0.001
L/mm	7.83	3.04	6.36	2.06	2738	< 0.001
S/L	0.80	0.19	0.85	0.15	3783	0.001
K_{trans}/min^{-1}	0.07	0.03	0.09	0.05	3176	< 0.001
K_{ep}/min^{-})	0.27	0.15	0.35	0.18	2968	< 0.001
V_e	0.29	0.15	0.26	0.15	4704	0.308

LNs: lymph nodes; S: short-axis diameter; L: long-axis diameter; S/L: short- to long-axis diameter ratio; IQR: inter-quartile range

n=35, N2 n=18; cM0 n=117, cM1 n=5)均符合纳入标准,确定DCE-MRI与病理结果相匹配淋巴结共203枚,转移淋巴结95枚,非转移淋巴结108枚。S≥5 mm淋巴结共138枚,转移淋巴结68枚,非转移淋巴结70枚;S<5 mm淋巴结共65枚,转移淋巴结27枚,非转移淋巴结38枚。

2.2 淋巴结径线及定量灌注参数测定结果

转移淋巴结的S、L均高于非转移淋巴结(P<0.01),其S/L、K_{trans}、K_{ep}则低于非转移淋巴结(P<0.01),而两者间V_e无统计学差异(P=0.308),见表1。K_{trans}的ROC曲线见图2,其曲线下面积(area under the curve, AUC)、诊断界值及其鉴别良恶性淋巴结的敏感性(sensitivity)、特异性(specificity)见表2。

2.3 以S=5 mm为界值淋巴结定量灌注参数测定结果

S≥5 mm转移淋巴结的K_{trans}、K_{ep}低于非转移淋巴结(P<0.001),V_e则高于非转移淋巴结(P=0.039);S<5 mm转移淋巴结K_{trans}值低于非转移淋巴结(P=0.001),二者间K_{ep}、V_e则无统计学差异(P>0.1),见表3。K_{trans}的ROC曲线及相关诊断界值见图2及表2。

表2 相关灌注定量参数ROC曲线分析结果

Table 2 ROC analyses of quantitative perfusion parameters

Lymph nodes	Parameter	AUC	Cutoff value	Sensitivity	Specificity
Total	K_{trans}	0.690	0.088	58.30%	78.90%
S≥5 mm	K_{trans}	0.675	0.088	57.10%	77.90%
S<5 mm	K_{trans}	0.732	0.087	60.50%	81.50%

S: short-axis diameter; AUC: area under the curve

表3 不同径线(以S=5 mm为界值)转移与非转移淋巴结定量灌注参数比较

Table 3 Quantitative perfusion parameters of metastatic and non-metastatic lymph nodes in different size (cutoff value S=5 mm)

Parameter	Metastatic LNs		Non-metastatic LNs		U	P
	Median	IQR	Median	IQR		
S≥5 mm	(n=68)		(n=70)			
K_{trans}/min^{-1}	0.07	0.03	0.09	0.05	1547.50	< 0.001
K_{ep}/min^{-1}	0.27	0.14	0.37	0.15	1151.50	< 0.001
V_e	0.31	0.15	0.25	0.14	1896.50	0.039
S<5 mm	(n=27)		(n=38)			
K_{trans}/min^{-1}	0.07	0.04	0.10	0.05	−3.459[1)]	0.001
K_{ep}/min^{-1}	0.30	0.15	0.32	0.15	401.50	0.138
V_e	0.24	0.15	0.28	0.20	432.50	0.284

LNs: lymph nodes; S: short-axis diameters; IQR: inter-quartile range; 1) t value

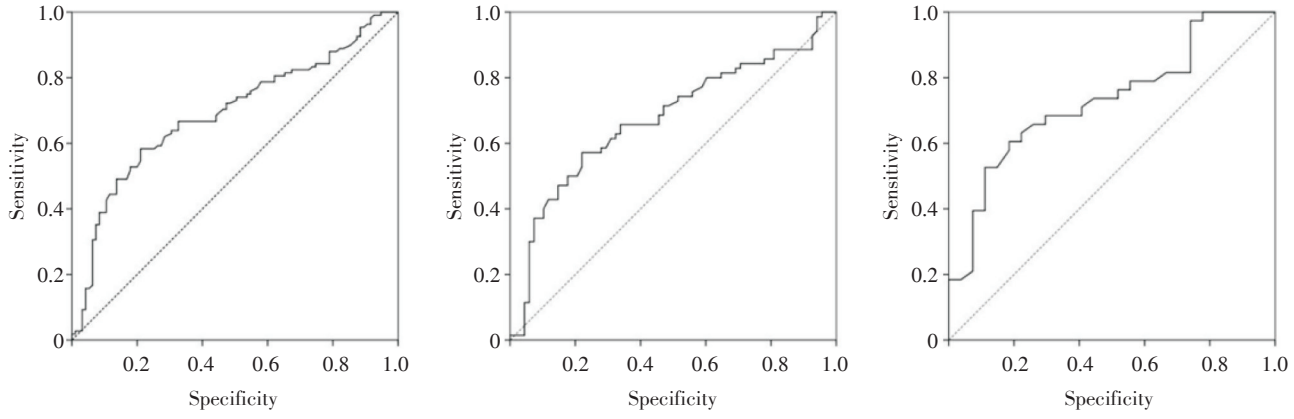

A：K_{trans} ROC of all lymph nodes；B：K_{trans} ROC of lymph nodes whose S >/=5 mm；C：K_{trans} ROC of lymph nodes whose S<5 mm.

图2　淋巴结K_{trans}的ROC曲线

Fig.2　Receive operating characteristic curves of K_{trans}

3　讨　论

美国国家综合癌症网络（National Comprehensive Cancer Network，NCCN）直肠癌指南明确指出，伴区域淋巴结转移的患者均推荐行术前新辅助治疗，并将盆腔MR检查作为直肠癌常规检查手段[1]。一项超过10000枚直肠癌淋巴结的病理研究显示，转移与非转移淋巴结的大小存在重叠，且50%以上转移淋巴结短径小于5 mm[8]。然而，直肠癌区域淋巴结良恶性的MR评价指标主要为淋巴结短径，现有不同研究的诊断界值各异[9, 10]，且由于转移淋巴结孤立肿瘤细胞及微转移所引起的形态学改变甚微[11]，故传统MRI难以对短径小于5 mm的淋巴结做出准确诊断[12]。DCE-MRI定量灌注参数能一定程度反映微小形态学改变所引起的功能改变，在评价淋巴结转移方面的研究与应用前景十分广阔。

一般而言，肿瘤细胞的生长赖于血管生成[13]，且新生肿瘤血管结构紊乱、内皮细胞异常[14]；由此可知，当发生淋巴结转移时，转移淋巴结微血管密度（microvessel density，MVD）增大[15]，血管渗透性升高，其微循环情况有别于非转移淋巴结。此前关于转移淋巴结微循环的研究大多基于病理学，已有相关研究[14-15]提示，转移淋巴结微血管渗透性及渗透面积均增大；但镜下病理表现为离体组织形态学判读，不足以充分反映活体组织微循环情况，尤其是微循环血流量。而DCE-MRI为新兴无创性检查，其定量灌注参数能反应活体组织微循环的真实情况，适用于术前评估。根据Tofts等提出的“二室相关”模型，K_{trans}反映的是微循环对比剂自血浆转移至EES的情况，其值大的小受微循环灌注量、微血管渗透性及渗透面积三个因素影响，且微循环高渗透状态时出现灌注受限（flow limit）[16]。本研究显示，直肠癌区域转移淋巴结K_{trans}值低于非转移淋巴结（0.07 min^{-1} VS 0.09 min^{-1}，P<0.001），提示转移淋巴结微循环血流量减少，血流速度减缓。Grøvik等[17]的研究显示，乏氧肿瘤组织灌注量减低，平均达峰时间延长，提示微循环血流缓慢；同时多项研究[9, 18]表明，转移淋巴结DCE-MRI定性参数时间-信号曲线（Time-contrast intensity curve，TIC）呈“缓慢流入、持续上升”表现，提示转移淋巴结微循环血流缓慢，均与本研究结论相一致。且本研究K_{trans}为定量参数，较定性参数TIC能进行更为精准的评价。根据2015年Meta分析提出的淋巴结短径诊断界值[19]，进一步以S=5 mm为界值的分组分析显示，针对不同径线的淋巴结，K_{trans}的诊断界值几乎相等（S ≥ 5 mmvs S < 5 mm 0.088 min^{-1} vs 0.087 min^{-1}），提示K_{trans}不受淋巴结径线影响，有较好的诊断稳定性及应用价值。无独有偶，Yan等[20]研究亦提示应用K_{trans}鉴别头颈部鳞癌转移淋巴结时，其值大小与淋巴结径线无关。在鉴别S < 5 mm的淋巴结方面，K_{trans}的诊断效能及特异性均较高（AUC 0.732，Specificity 81.5%），对于治疗前无创评估短径较小的淋巴结有较为可观的帮助。

V_e为单位体积组织EES容积，其值的大小取决于细胞增殖与坏死的双重作用[21, 22]。本研究显

示,当S≥5 mm时,转移淋巴结V_e值大于非转移淋巴结(0.31 vs 0.25, P=0.039),而当S<5 mm时,二者的V_e值则无统计学差异(P=0.284)。这可能是由于当转移淋巴结径线较小时,肿瘤细胞以增殖为主,细胞排列密集,细胞间尚未形成微坏死灶;而非转移淋巴结内由于存在大量淋巴细胞[15],细胞排列亦较为密集,故二者的V_e值并无明显差异。随着肿瘤细胞进一步增殖,淋巴结径线增大,但由于转移淋巴结微循环缓慢,其内逐渐出现形态学上难以观察的微坏死,导致细胞间隙增大,V_e值升高,Yan等[20]及Yu等[23]的研究结论亦可支持该观点。K_{ep}为对比剂经EES回流入血浆的速率常数,虽然主要反应微血管的渗透性,但根据Tofts等[16]所构的模型,$K_{ep}=K_{trans}/V_e$,其值受K_{trans}及V_e的双重影响,变异较大,个体差异尚需进一步研究证实。

值得注意的是,本研究的结果几乎与Yu等[23]的研究结果相悖,Yu等[23]的研究显示,转移淋巴结K_{trans}、V_e均大于非转移淋巴结(P<0.001),但二者的K_{ep}无差异。研究间出现这种差异的原因可能在于Yu等[23]的研究仅纳入直肠系膜内短径大于5 mm的淋巴结,数量较少,且仅勾画淋巴结最大层面,同时,选择髂血管构建AIF模型是否适合淋巴结的建模分析尚需进一步讨论。本研究则着眼于评价直肠癌区域淋巴结,尤其是短径小于5 mm的小淋巴结,且手动勾画淋巴结全层进行分析,对淋巴结的整体评价相对较为客观。本研究亦存在一些不足,由于直肠癌根治术并未常规清扫髂血管旁淋巴结,故本研究未纳入髂血管旁淋巴结进行分析。此外,本研究Gd-DTPA的注射剂量参考相关研究[20, 23]设定为0.1 mmol/kg,但注射速率各相关研究间[20, 23-24]略有差异,本研究Gd-DTPA注射速率为3.0 mL/s,满足DCE-MRI灌注分析要求,但对于灌注参数的影响尚需进一步研究探讨。

综上所述,DCE-MRI定量灌注参数K_{trans}可用于鉴别直肠癌区域淋巴结良恶性,且在鉴别短径小于5 mm的小淋巴结方面具有较高的诊断效能及特异性,这将有助于术前准确评估直肠癌区域淋巴结,以辅助临床制定更为合理的直肠癌个体化治疗方案。

参考文献

[1] National Comprehensive Cancer Network. Rectal Cancer Version 3.2017). Avarlable at https://www.nccn.org/professtionals/physician-gls/f-gurdelnes. asp. Accessed August 15,2017.

[2] Chen W, Zheng R, Baade PD, et al. Cancer statistics in China, 2015[J]. CA Cancer J Clin, 2016, 66(2): 115-132.

[3] Li XT, Sun YS, Tang L, et al. Evaluating local lymph node metastasis with magnetic resonance imaging, endoluminal ultrasound and computed tomography in rectal cancer: A meta-analysis[J]. Colorectal Dis, 2015, 17(6): O129-O135.

[4] Mizukami Y, Ueda S, Mizumoto A, et al. Diffusion-weighted magnetic resonance imaging for detecting lymph node metastasis of rectal cancer[J]. World J Surg, 2011, 35(4): 895-899.

[5] Collins DJ, Padhani AR. Dynamic magnetic resonance imaging of tumor perfusion. approaches and biomedical challenges[J]. IEEE Eng Med Biol Mag, 2004, 23(5): 65-83.

[6] Yao WW, Zhang H, Ding B, et al. Rectal cancer: 3D dynamic contrast-enhanced MRI; Correlation with microvascular density and clinicopathological features[J]. Radiol Med, 2011, 116(3): 366-374.

[7] Gollub MJ, Gultekin DH, Akin O, et al. Dynamic contrast enhanced- MRI for the detection of pathological complete response to neoadjuvant chemotherapy for locally advanced rectal cancer[J]. Eur Radiol, 2012, 22(4): 821-831.

[8] Langman G, Patel A, Bowley DM. Size and distribution of lymph nodes in rectal cancer resection specimens[J]. Dis Colon Rectum, 2015, 58(4): 406-414.

[9] Vag T, Slotta-Huspenina J, Rosenberg R, et al. Computerized analysis of enhancement kinetics for preoperative lymph node staging in rectal cancer using dynamic contrast- enhanced magnetic resonance imaging[J]. Clin Imaging, 2014, 38(6): 845-849.

[10] Doyon F, Attenberger UI, Dinter DJ, et al. Clinical relevance of morphologic MRI criteria for the assessment of lymph nodes in patients with rectal cancer[J]. Int J Colorectal Dis, 2015, 30(11): 1541-1546.

[11] Sobin LH, Gospodarowicz MK, Wittekind C, et al. TNM classification of malignant tumors[M]. 7th ed. Heiderberg: Springer- Verlag, 2009:93-95.

[12] Kim JH, Beets GL, Kim MJ, et al. High-resolution MR imaging for nodal staging in rectal cancer: Are there any criteria in addition to the size?[J]. Eur J Radiol, 2004, 52(1): 78-83.

[13] Choi HJ, Hyun MS, Jung GJ, et al. Tumor angiogenesis as a prognostic predictor in colorectal carcinoma with special reference to mode of metastasis and recurrence[J]. Oncology, 1998, 55(6): 575-581.
[14] Jain RK. Normalization of tumor vasculature: An emerging concept in antiangiogenic therapy [J]. Science, 2005, 307(5706): 58-62.
[15] Kwee TC, Basu S, Torigian DA, et al. Defining the role of modern imaging techniques in assessing lymph nodes for metastasis in cancer: evolving contribution of PET in this setting[J]. Eur J Nucl Med Mol Imaging, 2011, 38(7): 1353-1366.
[16] Tofts PS, Brix G, Buckley DL, et al. Estimating kinetic parameters from dynamic contrast- enhanced T1-weighted MRI of a diffusable tracer: Standardized quantities and symbols[J]. J Magn Reson Imaging, 1999, 10(3): 223-232.
[17] Grøvik E, Redalen KR, Storås TH, et al. Dynamic multi-echo DCE- and DSC-MRI in rectal cancer: Low primary tumor Ktrans and ΔR2* peak are significantly associated with lymph node metastasis[J]. J Magn Reson Imaging, 2017, 46(1): 194-206.
[18] Fischbein NJ, Noworolski SM, Henry RG, et al. Assessment of metastatic cervical adenopathy using dynamic contrast-enhanced MR imaging[J]. AJNR Am J Neuroradiol, 2003, 24(3): 301-311.
[19] Li XT, Sun YS, Tang L, et al. Evaluating local lymph node metastasis with magnetic resonance imaging, endoluminal ultrasound and computed tomography in rectal cancer: A meta-analysis[J]. Colorectal Dis, 2015, 17(6): O129-O135.
[20] Yan S, Wang Z, Li L, et al. Characterization of cervical lymph nodes using DCE-MRI: Differentiation between metastases from SCC of head and neck and benign lymph nodes [J]. Clin Hemorheol Microcirc, 2016, 64(2): 213-222.
[21] Langer DL, van der Kwast TH, Evans AJ, et al. Prostate tissue composition and MR measurements: Investigating the relationships between ADC, T2, K(trans), v(e), and corresponding histologic features[J]. Radiology, 2010, 255(2): 485-494.
[22] Choi HS, Kim AH, Ahn SS, et al. Glioma grading capability: Comparisons among parameters from dynamic contrast-enhanced MRI and ADC value on DWI[J]. Korean J Radiol, 2013, 14(3): 487-492.
[23] Yu X, Wen L, Hou J, et al. Discrimination of metastatic from non-metastatic mesorectal lymph nodes in rectal cancer using quantitative dynamic contrast-enhanced magnetic resonance imaging[J]. J Huazhong Univ Sci Technolog Med Sci, 2016, 36(4): 594-600.
[24] Kim SH, Lee JM, Gupta SN, et al. Dynamic contrast-enhanced MRI to evaluate the therapeutic response to neoadjuvant chemoradiation therapy in locally advanced rectal cancer[J]. J Magn Reson Imaging, 2014, 40(3): 730-737.

（编辑　王晓鹰）

（上接第899页　from page 899）

2012, 114(6): 585-589.
[14] Jennett B, Bond M. Assessment of outcome after severe brain damage[J]. Lancet, 1975, 1(7905): 480-484.
[15] Singhal A, Adirim T, Cochrane D, et al. Pediatric patients with poor neurological status and arteriovenous malformation hemorrhage: An outcome analysis[J]. J Neurosurg Pediatr, 2011, 7(5): 462-467.
[16] Toso PA, Gonzalez AJ, Perez ME, et al. Clinical utility of early amplitude integrated EEG in monitoring term newborns at risk of neurological injury[J]. J De Pediatr, 2014, 90(2): 143-148.
[17] Thorngate L, Foreman SW, Thomas KA. Quantification of neonatal amplitude-integrated EEG patterns[J]. Early Human Devel, 2013, 89(12): 931-937.
[18] Niemarkt HJ, Andriessen P, Peters CHL, et al. Quantitative analysis of amplitude-integrated electroencephalogram patterns in stable preterm infants, with normal neurological development at one year[J]. Neonatology, 2010, 97(2): 175-182.
[19] Soubasi V, Mitsakis K, Sarafidis K, et al. Early abnormal amplitude- integrated electroencephalography (aEEG) is associated with adverse short-term outcome in premature infants[J]. Eur J Paediatr Neurol, 2012, 16(6): 625-630.

（编辑　刘清海）